

The Structure, Composition, and Conditions of Generation for the Early Cretaceous Mongolia–East-Transbaikalia Volcanic Belt: The Durulgui–Torei Area (Southern Transbaikalia, Russia)

F. M. Stupak*, E. A. Kudryashova, V. A. Lebedev, and Yu. V. Gol'tsman

*Institute of Geology of Ore Deposits, Petrography, Mineralogy, and Geochemistry,
Russian Academy of Sciences (IGEM RAS), Staromonetnyi per., 35, Moscow, 119017 Russia*

*e-mail: fms38@mail.ru

Received April 25, 2016

Abstract—A system of variously sized basins filled with sediments and volcanic rocks was formed during Late Mesozoic time in Transbaikalia and adjacent areas of Mongolia and China. Magmatic formations are concentrated in three major volcanic belts: the Mongolia–West-Transbaikalia (MWT), the Mongolia–East-Transbaikalia (MET), and the Great Xing'an belt (GX). This paper presents a detailed description of the Early Cretaceous volcanism of the little-known MET belt within its Durulgui–Torei area, in particular, the Torei Lava Field (TLF) and a comparison between this and the same-age volcanism in the two other adjacent belts.

DOI: 10.1134/S0742046318010074

INTRODUCTION

During Late Mesozoic time the area of Transbaikalia and adjacent areas in Mongolia and China were an arena of intensive rifting and associated volcanism. These processes became especially spectacular and wide ranging in the Early Cretaceous, when numerous basins and fields of volcanogenic rocks of various sizes were formed in this area. They are shown in the area restricted within 108°–126° E and 42°–56° N in Fig. 1.

An analysis of this figure shows the existence of three well-separated and long sets of different-sized sedimentation and volcanogenic structures in the space between Lake Baikal in the northwest and the Sung-Liao Basin in the southeast. A large portion of the volume of these sets is occupied by volcanic rocks, thus classifying these sets as volcanic belts. The Cretaceous section of the area contains three such belts: the Great Xing'an (GX), the Mongolia–East-Transbaikalia (MET), and the Mongolia–West-Transbaikalia (MWT) belt. Some researchers combine the rocks of the two first belts together with the preceding Middle to Late Jurassic units to form the Upper Amur volcano-plutonic belt (Gordienko et al., 2000).

The three belts have similar external characteristics and primarily differ in the degree of knowledge about them. The GX belt is best understood (Zhang et al., 2008a, 2008b, 2010; Xu et al., 2013, among others). The belt contains abundant volcanic rocks of both moderate and normal alkalinity. The geodynamic setting of the Great Xing'an belt is open to debate; how-

ever, many researchers believe that this belt was a suprasubduction feature during Early Cretaceous time. It is a major volcanic province that was formed during the subduction of the Paleo-Pacific plate under the Eurasian continent; the process was accompanied by lithospheric thinning and an uplift of asthenospheric material.

The MWT belt is also well known, mostly concerning its largest, volcanic, West Transbaikalian region (Yarmolyuk et al., 1995, 1998; Vorontsov et al., 2002; Vorontsov and Yarmolyuk, 2007, among others). These authors support the hypothesis that the MWT volcanic rocks are intraplate in origin, which were due to the ascent of mantle plumes generated by the Central Asian hot mantle field controlling their origin and evolution.

The MET belt, which has abundant traces of the Early Cretaceous volcanism, is much less known compared with its neighbors. There are few data concerning the geological structure of dominantly basaltic volcanic fields and regions of the belt, concerning the time and peculiarities of their formation, and concerning the geochemical and isotope characteristics of their rocks. In this connection it is of interest to quote the data to be presented below that we obtained when studying the Torei Lava Field (TLF), which is a typical volcanic field in the MET belt.

This paper presents data on the geological structure of basaltic volcanic areas and fields in the Mongolia–East-Transbaikalia volcanic belt, as well as our own

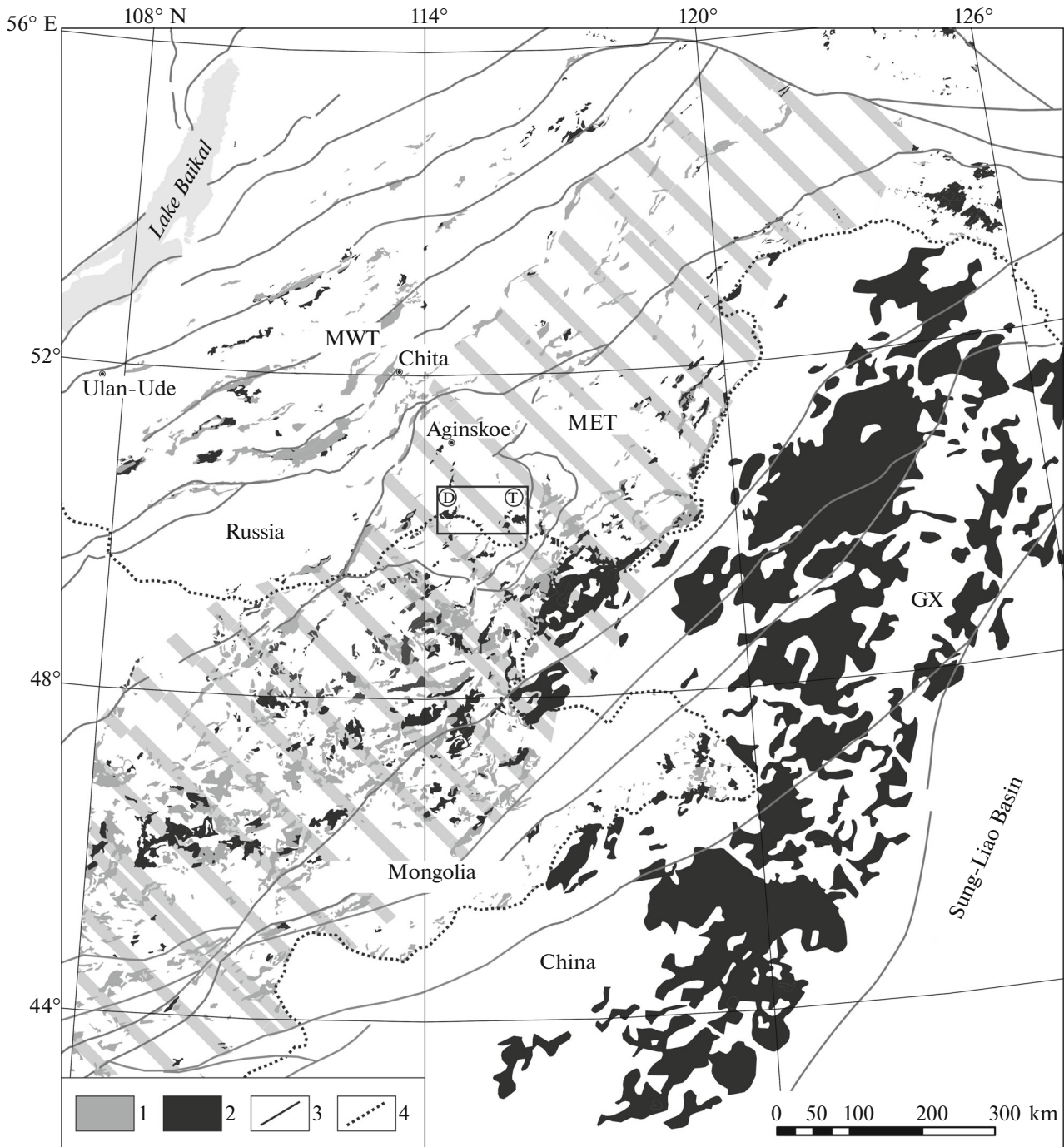


Fig. 1. A map showing the location of Early Cretaceous rocks in Transbaikalia and adjacent areas of Mongolia and China. This map is based on the *State Geological map of the Russian Federation* at a scale of 1 : 1000000 (third generation, fields N-49, N-50, N-51, M-49, M-50, M-51); the *Geological Map of Mongolia* at a scale of 1 : 1000000 (fields M-49, M-50, L-49, L-50, K-49), 2001; the *Geological Map of the Amur Area and Adjacent Territories* at a scale of 1 : 2500000 (*Geologicheskaya ...*, 1998); as also on (Zhang et al., 2008b, 2010; Xu et al., 2013). The fault network is after the *Tectonic Map of Central Asia and Adjacent Areas* (the international project *Atlas of Geological maps for Central Asia and Adjacent Areas* at a scale of 1 : 2500000, 2008). (1) sedimentary Cretaceous rocks, (2) Early Cretaceous volcanic fields, (3) major faults, (4) state borders. Volcanic belts: (GX) Great Xing'an, (MET) Mongolia–East-Transbaikalia (shaded by grey bands), (MWT) Mongolia–West-Transbaikalia; basins: (T) Torei, (D) Durulgui.

data on the geochemical and isotope features in the composition of volcanic rocks in a lava field of the belt. An analysis of these data led us to the conclusion about the conditions that prevailed during the formation of these rocks and about their ages. The goal of the present paper is to present evidence for our inference about the geotectonic setting of the MET belt.

A GENERAL DESCRIPTION OF THE TLF AND A BRIEF HISTORY OF ITS STUDY

The Torei Lava Field is situated among the low-hill steppe plains of the southern Transbaikalia, in the area of the Torei Lakes (Fig. 2). The various unconsolidated Cenozoic deposits that are abundant there, as well as the Lakes water, cover much of this field; we deduced its probable boundaries, as shown in the figure, from an interpretation of geophysical data. The total area of the field is 800 km²; the exposed part is approximately 400 km², with the rest being hidden by water and drift. Since the average thickness of the lava field is 600 m, its volume might reach 500 km³.

The lava field is exposed best in the northern part of the basins, where both of the Torei Lakes lie, as they are incised into a relatively high uplifted (by approximately 100 m) neotectonic block. The basement for the Torei lavas and the terrigenous sedimentary rocks that are interbedded with these is, according to (*Geologicheskaya ...*, 1989; *Geologicheskoe ...*, 1997; *Gosudarstvennaya ...*, 2010), sedimentary deposits that mostly date back to the Middle–Upper Devonian. The nearest periphery of the field and the fault zones that bound it contain only chlorite–sericite–quartz–feldspar schists.

The first evidence for the presence of young volcanic rocks in the Torei Lakes area became available in the 1920s (in the manuscripts of the geologists P.P. Sushchinskii, S.A. Muzylev, V.N. Rudnev, and others). S.A. Muzylev made a map of the TLF at a scale of 1 : 200 000 in 1929, which showed the main concepts of the contemporary geologists on the TLF volcanism: its young (Tertiary or Early Quaternary) age and a moderate (100 m) thickness of the lava field overlying Tertiary conglomerates. These are supplemented with data on “basaltic andesite” and “andesitic” chemical composition of the rocks, and on the presence of bipyroxene varieties (Egorova, 1932).

Later, the TLF was mostly studied during the making of geological maps at a scale of 1 : 200 000 (field M-50-XIV). The lavas and terrigenous deposits in the Torei Lakes area were classified in these maps as belonging to the Lower Cretaceous Turga Formation in the regional stratigraphic scheme for the southeastern Transbaikalia. The age of rocks in this formation is based on paleontological findings.

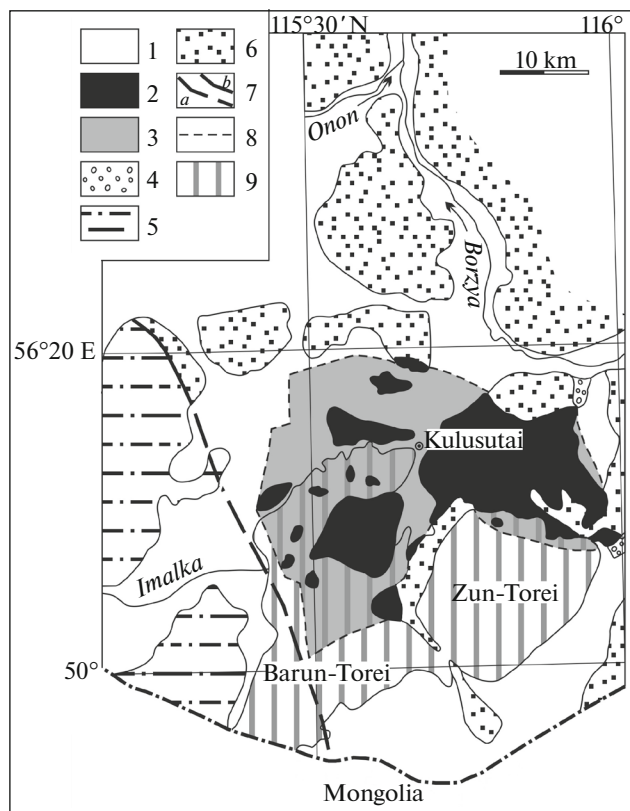


Fig. 2. The location and geological surroundings of the Torei Lava Field after (*Geologicheskaya ...*, 1989) with simplifications. (1–6) rocks: (1) Cenozoic, mostly unconsolidated Quaternary, (2–3) Early Cretaceous volcanogenic rocks of the Torei Field (2 exposed, 3 buried), (4) Early Cretaceous sediments of the Turga Formation, (5) Triassic sediments, (6) Paleozoic (Silurian to Carboniferous) metasedimentary rocks; (7) faults; (8) outline of the lava field; (9) lakes.

THE TLF STRUCTURE

In spite of the seeming uniformity of the TLF as a set of superimposed lava flows, its structure clearly shows three larger blocks (or segments) as deduced on the basis of several distinguishing features: the Western, the Central, and the Eastern blocks (Fig. 3). These blocks are separated by major faults, the north–south trending Teli–Kulusutai fault and the northwest trending Kuku–Hadan–Narin–Hundui fault. Narrow and long schist blocks that belong to the TLF basement are exposed at the surface in the zones of these faults.

The Western (or Barun-Torei) Block occupies over half of the entire TLF area. It extends in the same direction as the fault that bounds it on the east for over 30 km with an average width of 15 km. Nearly three-fourths of its area is covered by the waters of Lake Barun-Torei and by unconsolidated Quaternary deposits, with the rest being composed of lavas that were effused both in subaerial and subaqueous conditions, with the latter prevailing. The ejecta of the

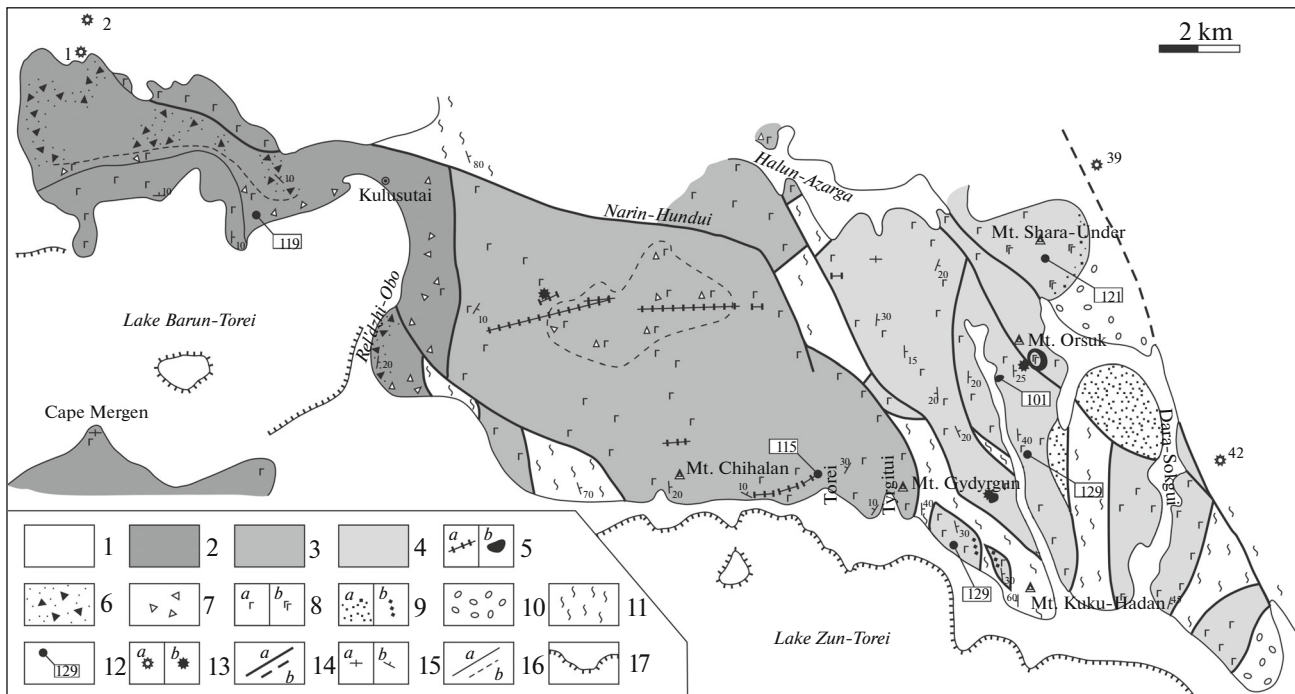


Fig. 3. A map showing the geological structure of the northern Torei Field. (1) Quaternary deposits; (2–4) blocks of the Field (2 Western, 3 Central, 4 Eastern); (5) post-effusive emplacements (*a* dikes; *b* sills and extrusions); (6, 7) subaqueous volcanic rocks (6 hyaloclastite, 7 core lava); (8) subaerial lavas with moderate (*a*) and high (*b*) degree of crystallinity; (9) fine-grained clastic rocks of the Eastern Block dispersed over the area (*a*) and in interbeds among basalts (*b*); (10) Turga conglomerate; (11) schist in the Field basement; (12) sampling sites for dating of volcanic rocks and ages (in Ma); (13) locations of the wells and their identification numbers (*a*), sites where megacrystals were found in volcanic rocks (*b*); (14) visible (*a*) and buried (*b*) faults; (15) horizontal (*a*) and dipping (*b*) attitudes of lava flows and clastic rocks; (16) age geological boundaries (*a*) and facies boundaries (*b*); (17) fragments of lacustrine shoreline.

underwater eruptions are dominated by core lavas (Stupak, 2000) with minor amounts of hyaloclastites and pillow lava. Subaerial lavas are not abundant within the Western Block.

The **Central** (or the Chihalan–Gydyrgun) Block is an area of the TLF that is nearly isometric in map view and stands high above the waters of Lake Zun-Torei. It is dominated by lavas of subaerial eruptions. The rock sequence contains alternating lava flows that are identical in structure. The number of flows in a single exposure can be ten or more, with individual flows being 1 to 10–12 or more meters thick. In the middle, the flows consist of dense grey lavas, while the lower and upper flows are composed of porous red-brown lavas.

The uppermost rocks in the lavas of the Central Block were found to contain small occurrences of subaqueous (core) lavas. When viewed with regard to structure, the lava sequence of the Central Block is a gently dipping brachysyncline, which is especially clearly seen in its southern, near-lake half where the flows dip toward the center of the feature.

Another characteristic of the Central Block consists in the presence of dikes. The dikes make two belts that strike nearly east–west, with the one extending

along the divide between the Narin-Hundui creek valley and Lake Zun-Torei and the other running along the northern periphery of that lake. The dikes are occasionally as long as 3 km with a thickness of 3 m and nearly vertical attitudes. With the exception of a single (diabase) dike, all the dikes are composed of porphyrites with phenocrysts of plagioclase, clinopyroxene and orthopyroxene, and titanomagnetite, which not infrequently reach the size of a megacrystal; one frequently encounters their glomeroporphyritic growths. Along with these, xenoliths of holocrystalline rocks of the dolerite aspect occur.

The **Eastern** Block of the TLF is situated between the Kuku-Hadan–Narin-Hundui fault, which was already referred to, and a fault that strikes in the same northwestern direction and bounds the area of volcanic rocks on the east (see Fig. 3). Further east, as far as the Borzinskoe and Ganga-Nor lakes, erosional truncations do not expose any Early Cretaceous volcanic rocks. It is only in some wells that were drilled in an adjacent area (on the east) near the above-mentioned fault (see Fig. 3, wells 39 and 42) that one encountered basaltic andesites that are probably edge parts of the TLF.

The Eastern Block consists of a series of smaller tectonic blocks that are generally elongate roughly northward. Most of these blocks are composed of sub-

Table 1. K–Ar datings for Durulgui–Torei rocks (MET volcanic belt)

Sample #	Rock	Sampling site	Potassium, % ($\pm\sigma$)	$^{40}\text{Ar}_{\text{rad}}$, ng/g ($\pm\sigma$)	Age, Ma ($\pm 2\sigma$)
Torei lava field					
77-0	BTA (stock)	Krementui Brook	2.35 ± 0.03	16.87 ± 0.10	101 ± 3
92-0	TA (dike)	Torei Brook	2.70 ± 0.03	22.13 ± 0.08	115 ± 3
55-0	BTA (later lavas)	Lake Barun-Torei	2.34 ± 0.03	19.90 ± 0.06	119 ± 3
84-0	TA (anamesite)	Mt. Shara-Under	2.46 ± 0.03	21.42 ± 0.11	121 ± 3
T-1	BTA (earlier lavas)	Lake Zun-Torei	2.02 ± 0.03	18.66 ± 0.06	129 ± 4
75-0	BTA (earlier lavas)	Krementui Brook	1.81 ± 0.02	16.76 ± 0.07	129 ± 3
Durulgui lava field					
96-40	BTA	SE Lake Tsagaan Nuur	1.42 ± 0.02	9.49 ± 0.04	94 ± 3
96-30	Diabase (sill)	Lake Daun-Bulak	2.18 ± 0.03	19.00 ± 0.07	121 ± 3
96-4-1	BA	NE Lake Nizhn. Kuchiger	1.00 ± 0.02	8.73 ± 0.04	122 ± 5
96-4	BTA	NE Lake Nizhn. Kuchiger	2.53 ± 0.03	22.45 ± 0.07	124 ± 3
96-25	TB	Western Lake Tsagaan Nuur	1.54 ± 0.02	13.93 ± 0.05	126 ± 3

The dates were determined in the Laboratory of Isotope Geochemistry and Geochronology, IGEM RAS (Moscow) using an Mi-1201 IG mass spectrometer. The bulk composition was analyzed. The concentration of Ar_{rad} was determined by isotope dilution using ^{38}Ar as the tracer, the concentrations of potassium were found by flame photometry. The age calculations used the following constants (Steiger and Jager, 1977): $\lambda_{\text{K}} = 0.581 \times 10^{-10} \text{ yr}^{-1}$, $\lambda_{\beta^-} = 4.962 \times 10^{-10} \text{ yr}^{-1}$, and $^{40}\text{K} = 0.01167$ (atm. %). Rocks: BA, basaltic andesite; TB, trachybasalt; BTA, basaltic trachyandesite; TA, trachyandesite.

aerial lavas, while several others contain sedimentary rocks associating with the lavas, with some of the blocks being composed of the schists of the TLF basement. Almost everywhere, the packets of lava flows are in monoclinic attitudes, dipping east at angles of 10° to 40° . One important feature of the Eastern Block consists in an abundance of terrigenous deposits. Two spatially isolated groups of terrigenous rocks have been identified: coarse-grained rocks (conglomerates) and fine-grained (mostly sandstone) rocks (see Fig. 3).

The Torei volcanic rocks when found within the Eastern Block also occur in the form of subvolcanic emplacements. Four such bodies occur there: a dike, the sill of Mt. Orsuk, and two extrusions (in the lower and in the upper part of the Krementui creek valley, see Fig. 3). All of these, except the last, are composed of porphyrites like those in the dikes of the Central Block; they contain the same megacrystals of mafic minerals and feldspar and fragments of light-colored dolerite-like (anamesite) rocks that are characteristic of the Shara-Under area. In contrast, the extrusion in the upper part of the Krementui creek valley is composed of core lavas that are widely abundant in the Western Block.

THE AGE OF THE TLF ROCKS

The authors of the most recent geological map (geolokarta-200) (*Geologicheskaya ...*, 2010) used determinations of faunistic and floristic units that are found in the terrigenous rocks of the Torei Basin to infer that these belong to the Turga Berriasian–Barremian biostratigraphic horizon.

The first isotope K–Ar datings of volcanogenic rocks sampled from the Torei and East Torei basins were given by V.F. Korolev (1962) without indicating the exact sampling sites. The ages were found to lie in the time span 198–122 Ma based on five samples. Somewhat later, L.F. Cherbyanova et al. (1966) gave the value 120 Ma as the age for the Western Block basalts.

Recently we obtained six dates at the Laboratory of Isotope Geochemistry and Geochronology (IGEM RAS), Moscow for TLF volcanic rocks using the K–Ar technique (Analyst V.A. Lebedev) (Table 1, see Fig. 3). All of these dates indicate an Early Cretaceous time of volcanic activity for the Torei Lakes area. The activity dates back to the Early Barremian on the scale of (Ogg et al., 2012), when the early lavas dated as 129 Ma were effused within the Eastern Block. Such lavas have not been detected in the rest of the TLF, while the Eastern Block contains their exposures in its southern half.

The rest of the TLF was formed by fissure eruptions in the middle of the Aptian. We found lavas of that age in the northern Eastern Block (the Shara-Under area) where they were dated as 121 ± 3 Ma (see Table 1). Judging from some indirect evidence, the TLF Central Block is entirely built by lavas of the same or a similar age, seeing that these lavas are penetrated by a porphyrite dike that was dated 115 ± 3 Ma (see Table 1). The Middle Aptian eruptions also built the lava sequence of the TLF Western Block, whose rocks were dated as 119 ± 3 Ma (see Table 1). The TLF formation was complete when small subvolcanic porphyrite intrusions were emplaced in the Middle Aptian

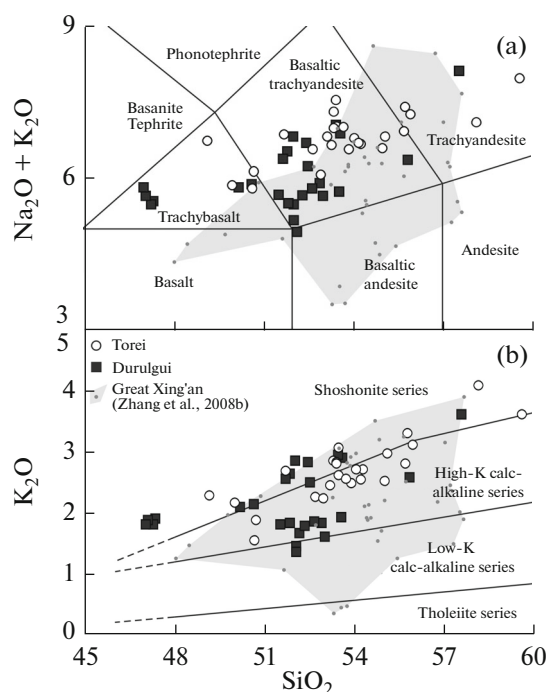


Fig. 4. The $(\text{Na}_2\text{O} + \text{K}_2\text{O})\text{--SiO}_2$ (Klassifikatsiya ..., 1997; Le Bas et al., 1986) (a) and the $\text{K}_2\text{O}\text{--SiO}_2$ (Peccerillo and Taylor, 1976) (b) diagrams for the MET Early Cretaceous volcanic rocks (Durulgui and Torei basins) and for the GX belt.

and core lavas were extruded at the end of the Albian (101 ± 3 Ma, see Table 1).

THE PETROCHEMICAL AND ISOTOPE GEOCHEMICAL FEATURES OF THE TLF VOLCANIC ROCKS

The analytical technique. We based our inferences about the geochemistry of the TLF volcanogenic rocks on 25 chemical analyses performed by the XRF method at the Vinogradov Institute of Geochemistry SB RAS (Irkutsk City) following (Afonin et al., 1984). The most representative of these analyses are listed in Table 2. Six samples from the TLF were analyzed by the ICP-MS technique to find the amounts of rare and rare-earth elements (see Table 2). We also used previously unpublished data, for comparison purposes, for Early Cretaceous (126–94 Ma, see Table 1) intermediate to basic effusive rocks sampled from the Durulgui Basin of the MET volcanic belt (see Fig. 1), which is the nearest from the west; the analyses were performed using the same techniques and at the same institute (see Table 2). Information on the geology of the Durulgui Basin can be found in (Stupak, 1999).

Data on the isotope composition of volcanic rocks sampled in the Torei and Durulgui basins are derived from the analyses that were performed in the Laboratory of Isotope Geochemistry and Geochronology

(IGEM RAS), Analyst Yu.V. Gol'tsman (Table 3). The isotope composition of Sr and Nd was studied using a Sector 54 multicollector thermal ionization mass spectrometer (Micromass) following the procedure outlined in (Chernyshev et al., 2012).

We also compared the Early Cretaceous volcanic rocks sampled in both basins of the MET volcanic belt with rocks from the GX volcanic belt, which have the same age and composition (Zhang et al., 2008b, 2010).

Petrochemistry. The TLF volcanic rocks are classified, by the concentrations of silica and alkalis, as belonging to the order of basic and intermediate rocks, to the suborder of moderately alkaline magmatic rocks of the potassium–sodium type (*Petrograficheskii ...*, 2009). Two-thirds of all TLF samples that are lavas when considered as a facies are diagnosed in the $(\text{Na}_2\text{O} + \text{K}_2\text{O})\text{--SiO}_2$ diagram (Klassifikatsiya ..., 1997) (Fig. 4a) as basaltic trachyandesites (shoshonites), while the others, which are shallow emplacements with cumulative phases, are classified as trachybasalts (potassium trachybasalts, occasionally hawaiites) and trachyandesites (latites). Although the TLF rocks tend toward potassium, the amount of Na_2O in them is nearly always greater than that of K_2O , with their ratio varying in the range from 1 to 2.

The $\text{K}_2\text{O}\text{--SiO}_2$ diagram (Peccerillo and Taylor, 1976) (see Fig. 4b) has the data points of the Torei volcanic rocks mostly plotting in the field of high potassium calc-alkaline, more rarely, shoshonite, series.

Overall, the TLF volcanic rocks show increased concentrations of components that belong to melanocratic rocks (wt %): MgO (2–6), $\text{Fe}_2\text{O}_{3\text{T}}$ (8–12), P_2O_5 (0.6–1.2), and TiO_2 (1.5–2.5) (see Table 2). The $\text{MgO}\text{--TiO}_2$, $\text{MgO}\text{--P}_2\text{O}_5$, and $\text{MgO}\text{--Fe}_2\text{O}_{3\text{T}}$ diagrams (Fig. 5) reveal the fact that the Torei lavas contain lower amounts of oxides of Ti, P, and Fe compared with the Durulgui lavas.

The volcanic rocks in the Durulgui Basin have the same age as the TLF rocks, and are similar to these both regarding their petrography and petrochemistry. The differences consist in a slightly lower alkalinity of the effusive rocks sampled in the Durulgui Basin (see Fig. 4). Considered in relation to the concentration of melanocratic components, the Durulgui volcanic rocks exceed the TLF rocks (see Fig. 5).

The Early Cretaceous volcanic rocks in the GX volcanic belt (Zhang et al., 2008b) are mostly similar (by their petrochemistry) to those sampled in the Torei and Durulgui basins of the MET belt. The lavas in the northern GX belt (the Genhe and Tahe groups) show the closest compositional similarity to the lavas sampled in the Durulgui and Torei basins, while those sampled in the southern GX belt (Zalute group), as represented by the dominant normal alkalinity varieties, show the greatest dissimilarity to the Durulgui and Torei lavas. Lower concentrations of K_2O classify the Zalute rocks as belonging to the low potassium calc-

Table 2. The chemical composition (wt %) and the composition of trace and rare-earth elements (ppm) in Early Cretaceous of the Durulgui–Torei area in the MET volcanic belt

	Torei lava field							Durulgui lava field							
	T-1	55-0	75-0	77-0	84-0	92-0	96-8	96-9	96-20	96-25	96-30	96-31	96-32	96-33	96-40
	BTA(Sh)	BTA(Sh)	BTA(Sh)	BTA(Sh)	TA(L)	TA(L)	BTA(Sh)	BTA(Sh)	BTA(M)	TB(P)	BTA(Sh)	BTA(Sh)	BTA(Sh)	TA(L)	BTA(M)
SiO ₂	53.23	52.50	51.49	53.79	54.95	54.92	50.83	51.94	49.84	46.6	51.92	52.63	52.20	56.68	51.20
TiO ₂	2.30	2.25	2.72	2.04	2.1	1.91	2.69	2.65	2.72	2.7	2.61	2.57	2.81	2.27	2.75
Al ₂ O ₃	15.68	15.58	14.92	15.46	15.8	15.84	15.10	15.23	14.84	15.46	15.36	14.89	14.50	14.7	15.04
Fe ₂ O _{3T}	9.38	10.43	10.37	10.01	9.97	9.12	11.37	10.53	11.28	13.75	10.86	10.10	10.22	8.82	11.27
MnO	0.10	0.17	0.10	0.15	0.14	0.14	0.15	0.10	0.17	0.2	0.13	0.13	0.13	0.14	0.14
MgO	3.80	3.65	3.45	3.10	1.47	2.82	3.75	2.48	3.56	5.26	3.48	3.62	3.40	2.6	3.44
CaO	6.74	6.27	7.13	5.59	5.66	5.6	7.32	7.05	6.92	7.18	6.89	6.19	6.33	4.55	7.04
Na ₂ O	4.02	3.70	3.72	3.74	4.05	4.01	3.57	3.68	3.53	3.57	3.67	3.90	3.98	4.41	3.76
K ₂ O	2.48	2.85	2.19	2.92	3.09	3.28	1.82	1.89	1.42	1.84	2.50	2.87	2.91	3.59	1.78
P ₂ O ₅	1.09	1.15	1.18	0.87	1.07	0.88	1.44	1.45	1.48	1.58	1.49	1.33	1.20	0.73	1.42
L.O.I.	1.26	1.49	2.69	2.34	1.6	1.46	1.99	2.99	4.27	2	1.06	1.76	2.36	1.44	2.04
Total	100.08	100.04	99.96	100.01	99.9	99.98	100.03	99.99	100.03	100.14	99.97	99.99	100.04	99.93	99.88
V	186	163	190	153	156	137	182	188	187	211	190	169	182	138	191
Cr	61.30	39.00	55.50	32.70	41.10	32.30	51.40	49.20	51.10	52.40	57.90	19.90	11.60	10.10	53.10
Co	25.90	25.30	27.20	22.10	22.00	20.00	28.80	21.20	26.60	33.70	28.00	23.60	21.60	15.00	28.80
Ni	36.40	23.30	28.20	18.20	19.90	18.20	25.40	21.80	25.80	39.10	31.90	21.90	16.10	8.25	26.80
Zn	142	132	156	121	117	114	161	141	178	168	164	166	167	159	163
Ga	24.00	21.40	23.60	20.20	22.90	21.60	24.30	24.20	24.70	23.40	24.80	24.90	24.80	24.50	24.20
Rb	52.80	52.90	37.20	85.10	60.40	77.70	38.50	75.20	38.80	35.60	49.40	61.20	57.30	77.00	56.60
Sr	957	922	955	614	913	767	1040	921	1020	912	994	960	909	755	889
Y	25.70	42.30	27.10	47.60	45.10	42.70	42.30	45.10	44.30	58.90	38.00	35.10	37.30	38.70	44.00
Zr	474	351	418	383	422	434	516	567	528	714	517	618	594	735	526
Nb	28.10	49.60	31.30	52.60	48.50	53.20	44.10	44.50	44.40	68.60	39.80	41.50	43.90	51.60	43.30

Table 2. (Contd.)

	Torei lava field						Durulgui lava field									
	T-1	55-0	75-0	77-0	84-0	92-0	96-8	96-9	96-20	96-25	96-30	96-31	96-32	96-33	96-40	
	BTA(Sh)	BTA(Sh)	BTA(Sh)	BTA(Sh)	TA(L)	TA(L)	BTA(Sh)	BTA(Sh)	BTA(M)	TB(P)	BTA(Sh)	BTA(Sh)	BTA(Sh)	TA(L)	BTA(M)	
Cs	20.40	0.64	14.80	9.53	1.23	4.44	5.69	3.04	1.70	0.35	1.37	1.71	1.62	1.74	1.49	
Ba	1010	1180	1010	946	1320	1100	1180	1290	1170	1310	1290	1400	1440	1800	1120	
La	74.10	57.90	65.60	47.90	63.60	58.60	80.60	84.00	81.90	89.10	81.20	89.30	95.10	103.00	76.30	
Ce	156	124	143	102.00	135	122	171	180	176	195	176	193	202	225	167	
Pr	19.40	15.60	17.80	12.50	16.50	15.20	21.20	23.30	23.10	25.40	22.70	24.10	24.60	26.40	21.10	
Nd	76.00	63.90	71.90	53.10	66.10	57.50	85.10	91.40	89.60	101.00	89.20	91.10	95.80	102.00	89.40	
Sm	15.00	14.50	15.70	11.80	13.60	11.70	15.50	17.80	15.90	20.20	17.50	15.80	16.90	17.50	18.20	
Eu	3.37	3.37	3.45	2.99	3.25	2.85	3.95	4.58	4.15	4.71	4.14	4.30	4.00	4.17	3.90	
Gd	9.70	10.80	10.40	10.00	10.60	10.70	13.10	13.70	13.80	15.90	12.50	13.00	13.20	14.00	14.10	
Tb	1.30	1.60	1.29	1.63	1.56	1.65	2.00	2.07	2.12	2.47	1.88	1.68	1.87	1.89	1.93	
Dy	5.67	8.16	6.16	8.53	8.45	7.92	8.64	9.33	8.86	11.70	7.95	7.19	7.80	8.12	8.99	
Ho	0.85	1.51	0.95	1.57	1.49	1.57	1.57	1.62	1.53	2.09	1.40	1.24	1.39	1.44	1.46	
Er	2.04	4.29	2.38	4.46	4.40	4.13	4.02	4.23	4.15	5.81	3.57	3.20	3.23	3.62	4.17	
Tm	0.28	0.60	0.29	0.59	0.57	0.53	0.48	0.51	0.47	0.75	0.46	0.39	0.44	0.51	0.55	
Yb	1.80	3.83	1.75	4.35	3.47	3.86	3.75	3.78	3.41	5.04	3.09	2.67	2.84	3.24	3.28	
Lu	0.25	0.56	0.27	0.65	0.56	0.59	0.52	0.56	0.47	0.78	0.43	0.44	0.43	0.47	0.50	
Hf	9.02	8.00	8.74	8.40	8.73	10.40	10.90	12.30	12.00	14.70	11.30	13.70	12.70	16.20	11.30	
Ta	1.43	2.77	1.75	2.97	2.67	2.96	2.47	2.42	2.47	3.50	2.14	2.19	2.08	2.48	2.26	
Pb	12.80	11.70	10.70	11.90	12.00	16.50	18.80	17.40	14.70	15.40	26.20	23.90	22.30	17.80	15.20	
Th	4.15	3.68	3.59	4.05	4.20	5.28	3.84	4.54	4.02	2.90	3.95	4.27	3.95	5.25	4.04	
U	1.36	1.08	1.14	1.18	1.30	1.48	1.19	1.30	1.22	0.83	1.22	1.22	1.17	1.52	1.15	

TLF: Western Block: aphyric subaqueous lavas on the northern shore of Lake Barun-Torei (55-0). Central Block: dikes in the valley Torei (92-0). Eastern Block: subaerial lavas (T-1 are from the section of a tectonic outlier west of the lower reaches of Kremenui Valley, 75-0 are from left bank of middle segment of the same valley, 84-0 anamesite from Mt. Shara-Under), subvolcanic rocks (77-0 a stock of aphyric core lavas in Kremenui Valley). DLF: effusive rocks (96-8, 96-9, 96-20, 96-25, 96-40); subvolcanic diabase from Daun-Bulak sill (96-30 melanocratic fine-grained, 96-31 meso-melanocratic fine-grained, 96-32 mesocratic medium-grained, 96-33 pegmatoidal). Rocks: BA, basaltic andesite; TB, trachybasalt (P, potassium trachybasalt); BTA, basaltic trachyandesite (Sh, shoshonite); TA, trachyandesite (L, latite).

Table 3. The isotope composition of Sr and Nd in Early Cretaceous Durulgui–Torei rocks (MET volcanic belt)

Sample	Rock	Sm, ppm	Nd, ppm	$^{147}\text{Sm}/^{144}\text{Nd}$	$^{143}\text{Nd}/^{144}\text{Nd}$	2σ	ϵ_{Nd} (MZ _t)	Rb, ppm	Sr, ppm	$^{87}\text{Rb}/^{86}\text{Sr}$	$^{87}\text{Sr}/^{86}\text{Sr}$	2σ	ϵ_{Sr} (MZ _t)
Torei lava field													
T-1	BTA(Sh)	12	72	0.1049	0.512606	6	0.9	56	1019	0.1598	0.705386	9	10.5
55-0	BTA(Sh)	11.3	58	0.1170	0.512586	23	0.2	55	923	0.1734	0.705511	7	12.2
Durulgui lava field													
96-20	BTA(M)	16	88	0.1106	0.512536	5	-0.8	41	1087	0.1095	0.705989	10	20.5
96-25	TB(P)	18	95	0.1146	0.512628	6	1.1	38	941	0.1155	0.705312	10	10.7

TB(P), potassium trachybasalt; BTA, basaltic trachyandesite (Sh, shoshonite; M, mugearite).

alkaline series. In addition, the Early Cretaceous GX volcanic rocks show generally lower concentrations of TiO_2 , P_2O_5 , and $\text{Fe}_2\text{O}_{3\text{T}}$, and higher MgO (see Fig. 5).

Geochemistry. The concentrations of trace elements and rare-earth elements (REE) in the TLF rocks are listed in Table 2 and shown in Fig. 6. The lava compositions are similar overall in their trace and rare-earth elements characteristics to ocean island basalts (OIB) (Sun and McDonough, 1989); however, at the same time they differ in the enrichment of large-ion lithophile elements, light REEs, most high field strength elements, and in the depletion (in the earlier lavas only) in heavy REEs and in some high field strength (Ti, Th) elements. In addition, they show a negative europium anomaly.

At the same time, the rocks of different-aged TLF groups, the earlier (129 Ma) rocks and the later (121–101 Ma) rocks, show certain geochemical differences. At the petrochemical level, differences such as these are poorly pronounced and are seen in the form of slightly higher concentrations of TiO_2 and lower con-

centrations of Al_2O_3 in the earlier lavas. At the trace-element level, the earlier lavas differ from the later in higher (by factors of 1.5–2) concentrations of ferrous elements, Cs, Sr, Zr, light REEs, and lower (by factors of 1.5–2) concentrations of Rb, Y, Nb, Ta, and heavy REEs (see Table 2).

The patterns of normalized concentrations of trace elements in the TLF rocks (see Fig. 6) shows the presence of positive anomalies of large-ion lithophile elements (Rb, Ba, and K) and negative anomalies in high field strength elements (Nb and Ta), which are characteristic of the earlier TLF lavas only. These patterns are similar to that for continental arc basalts (CAB) (Kelemen et al., 2003); this, when combined with a well-pronounced Nb–Ta trough and a high $(\text{La}/\text{Yb})_n = 25\text{--}28$, makes the earlier TLF lavas more similar to the CAB rocks. The TLF trends in the middle of the plot run as a narrow band along the trend line of average OIB compositions as far as their negative Ti anomaly, with the trend of the earlier lavas persistently remaining higher. The segment of the heavy REEs shows a

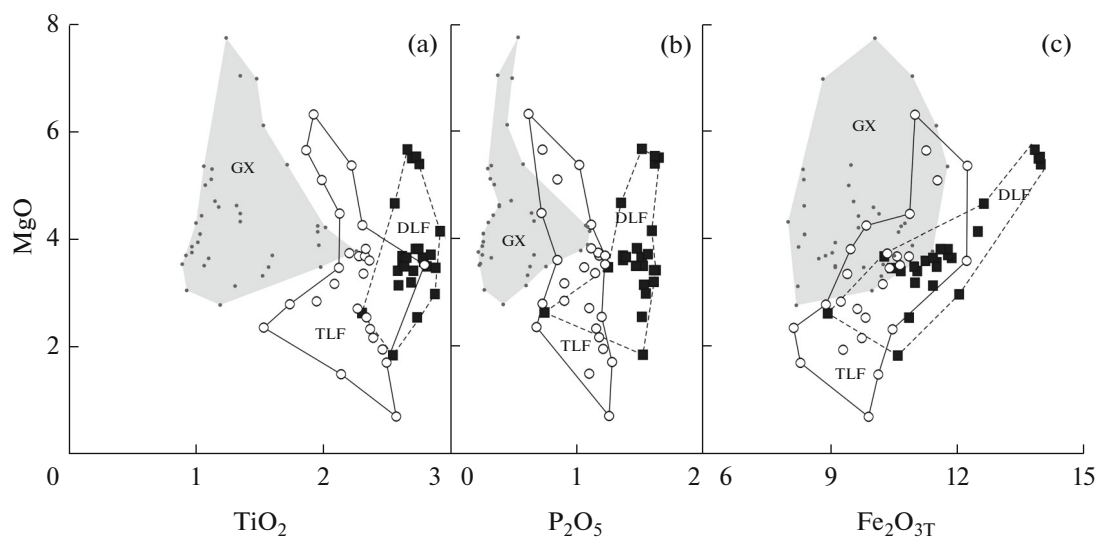


Fig. 5. The MgO versus TiO_2 (a), P_2O_5 (b), and $\text{Fe}_2\text{O}_{3\text{T}}$ (c) diagrams for MET Early Cretaceous intermediate to basic rocks (Durulgui and Torei basins) and for the GX belt. For the legend, see Fig. 4. Contours mark the Durulgui (DLF) and the Torei (TLF) lava fields.

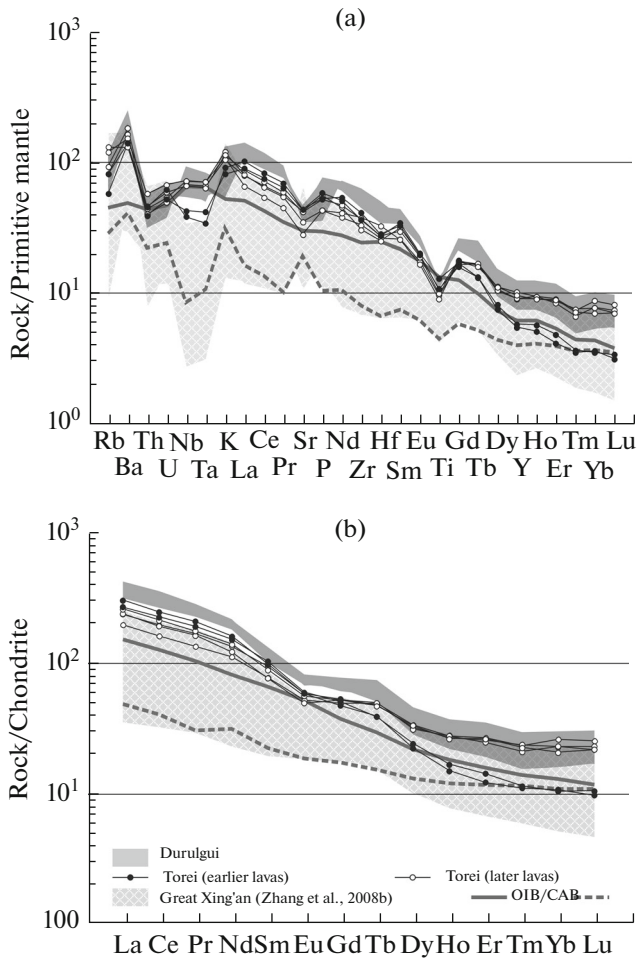


Fig. 6. The trace (a) and rare-earth (b) elements patterns normalized after (Sun and McDonough, 1989) for the MET Early Cretaceous intermediate to basic rocks (Durulgui–Torei area) and for the GX belt. Average basalt compositions: ocean islands (OIB) and continental arcs (CAB) are after (Sun and McDonough, 1989; Kelemen et al., 2003).

splitting of the common TLF compositional band into two parts. The upper of these, which represents the later lavas, extends above the OIB trend nearly parallel to it, while the lower, which corresponds to the composition of the earlier lavas, is inclined more steeply relative to this trend and intersects it, coalescing with the trend of average CAB compositions at its termination.

Comparison of the trace-element compositions of the Durulgui and Torei lavas with those of the GX lavas (Zhang et al., 2008b) reveals the fact that the latter show overall lower concentrations of most elements; they have a well-pronounced Ta–Nb minimum and an Sr maximum. The spectra of element distribution in the MET volcanic rocks show the greatest similarity to the spectra of volcanic rocks sampled in the northern GX belt (the Genhe and Tahe groups). The volcanic rocks in the southern GX belt (the Zalute

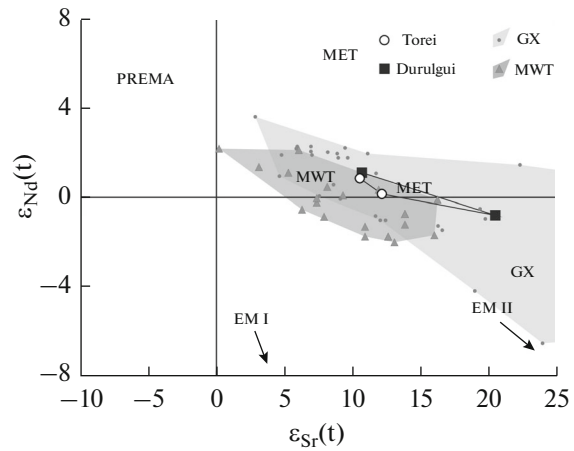


Fig. 7. The $\epsilon_{Nd}(t)$ – $\epsilon_{Sr}(t)$ diagram for isotope compositions of Early Cretaceous intermediate to basic rocks (the MET, MWT, and GX volcanic belts). The GX compositions are after (Zhang et al., 2008b), the MWT (Dzhida, Tugnui-Khilok, and Uda sectors) are after (Yarmolyuk et al., 1998; Vorontsov et al., 2002; Vorontsov and Yarmolyuk, 2007). Mantle sources (Zindler and Hart, 1986): PREMA stands for a moderately depleted (prevalent) mantle; EM I and EM II denote an enriched mantle.

group) are characterized by considerable depletions in most trace elements and light REEs compared with the rocks of both above-mentioned MET basins.

The isotope composition of Sr and Nd. The data on the isotope compositions of Sr and Nd in the Torei and Durulgui volcanogenic rocks are listed in Table 3 and shown in Fig. 7.

The positions of data points for the isotope compositions of volcanic rocks sampled in the MET Durulgui and Torei basins when plotted in the $\epsilon_{Nd}(t)$ – $\epsilon_{Sr}(t)$ coordinates (see Fig. 7) provide evidence of their positions within the mantle series between the PREMA and EM II sources (Zindler and Hart, 1986). They make a trend within the limits $10 < \epsilon_{Sr}(t) < 21$ and $-1 < \epsilon_{Nd}(t) < 1.5$, which lies between similar trends of the Early Cretaceous volcanic rocks for GX (Zhang et al., 2008b) and for MWT (Yarmolyuk et al., 1998; Vorontsov et al., 2002; Vorontsov and Yarmolyuk, 2007) belts, and which is roughly parallel to them. The volcanic rocks of all the three belts are moderately enriched in radiogenic strontium $0 < \epsilon_{Sr}(t) < 25$ (up to 50 in some GX rocks) and show a gentle depletion in radiogenic neodymium ($-2 < \epsilon_{Nd}(t) < 4$, with -7 in some rare GX rocks).

DISCUSSION

The information presented above on the geology of the TLF, and on the age and composition of the constituent rocks, suggest several considerations bearing on the character and manifestations, petrogenetic and geodynamic features of the Early Cretaceous volca-

nism as occurred in the Durulgui and Torei basins of the MET volcanic belt.

The sections of the Early Cretaceous sedimentary–volcanogenic rock sequences that fill the Torei and Durulgui basins contain products of intermediate to basic magmas that were discharged in water. These are also known in many other basins of the Early Cretaceous MWT and MET volcanic belts. Such products make the subaqueous triad “hyaloclastite–core lavas–pillow lavas” (Stupak, 2002). Hyaloclastites were not previously identified as a special variety of effusive clastic rocks (*Petrograficheskii ...*, 2009) in the Russian part of the MET belt. They were treated as pyroclastic rocks due to explosive activity on central-type volcanoes and at the same time as a weighty argument for the existence of the latter. However, it should be said that the Russian part of the MET belt has not been found to contain reliably identified major volcanic edifices of the central type that were erupting intermediate to basic lavas during Early Cretaceous time. They also seem to be absent from the Mongolian part of this belt, judging from some review papers (Frikh-Khar and Luchitskaya, 1978; *Vulkano-plutonicheskie ...*, 1991). It thus appears that the identification of a hyaloclastic origin for volcano-clastic rocks in the Early Cretaceous fields found in the Durulgui (Stupak, 1999), Torei (the present paper), and several other Early Cretaceous basins in the Transbaikalia (Stupak, 2012) must, on the one hand, argue against the concept of their relationships to central-type volcanoes and, on the other, highlight fissure eruptions as occurrences that play the leading part in the generation of such fields.

It has been noted that the TLF volcanic rocks are enriched in LILE, HFSE, and LREE. It was shown earlier (Zhang et al., 2008b) that a similar enrichment is typical of the GX volcanic rocks. These authors used the Rb/Y–Zr/Y diagram to show that a similar enrichment was occurring in subduction zones or in situations when melts were contaminated with crustal material. When plotted in that diagram (Fig. 8), the Durulgui–Torei volcanic rocks tend toward the trend of intraplate enrichment. The intrachamber evolution of magma melts occurred in a similar manner in both of these cases, namely, under the conditions of crystallization differentiation. This is corroborated, apart from the chemical evolution of the rocks, by the presence of cumulative rocks in the TLF porphyrite intrusions, as well as in the Durulgui lavas; these rocks are phenocrysts (which are occasionally as large as megacrysts) and their glomerular growths.

The Early Cretaceous volcanic rocks of intermediate to basic composition in the GX volcanic belt are presently considered as suprasubduction formations that were due to the Paleo-Asian (Izanagi) plate that subducted under the Eurasian continent (Zhang et al., 2008b, 2010; Xu et al., 2013). In contrast, the MWT intermediate to basic volcanic rocks that are similarly

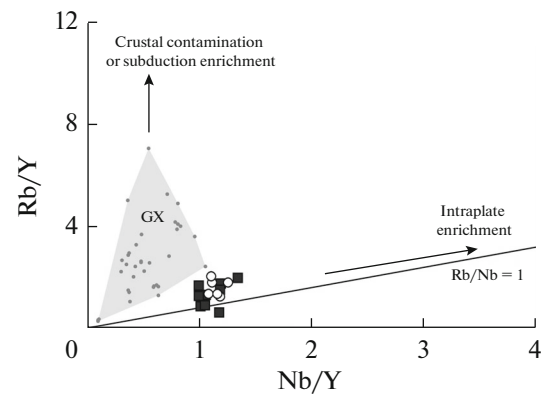


Fig. 8. The Rb/Y–Nb/Y diagram (Zhang et al., 2008b) for the Early Cretaceous intermediate to basic rocks in the MET belt (Durulgui–Torei area) and for the GX belt. For legend see Fig. 4.

dated are considered as deriving from intraplate plume magmatism (Yarmolyuk et al., 1998; Yarmolyuk and Kovalenko, 2003; Vorontsov et al., 2002; Vorontsov and Yarmolyuk, 2007). Since the Durulgui–Torei area, as well as the MET belt itself, lie between the two above belts, magmatic formations due to both types of geodynamic setting can have been produced in the area.

Our data on petrochemistry, the concentrations of trace and rare-earth elements, and the isotopes of Sr and Nd for the Durulgui–Torei volcanic rocks, provide evidence of prevailing products of plume volcanism. It is only the earlier lavas of the Torei Field that exhibit definite features (the Nb–Ta trough, the character of the trace and rare-earth elements, and depletion in heavy REEs) that indicate their deviation toward island-arc formations.

One can get a fair idea of the relationships between both types of geodynamic setting by looking at the Nb/La–Ba/La diagram (Fig. 9a). The compositional data points for the suprasubduction rocks in all groups of the GX volcanic belt make a compact area extending along the horizontal axis, with the Nb/La ratio below 0.5. The band-shaped area of the MET volcanic rocks dips steeply relative to the GX area, intersecting it in the starting part. The separation and the different orientations shown by the compositions of both genetic types are also clearly seen in the Ba/Nb–SiO₂ diagram (see Fig. 9b). It follows that the MET Durulgui–Torei volcanic rocks are intraplate in origin and probably originated from the action of a mantle hotspot at the boundary with the region of supra-subduction volcanism.

CONCLUSIONS

The above information on the age, conditions of occurrence, and composition of the Early Cretaceous volcanic rocks sampled in the Durulgui–Torei area of

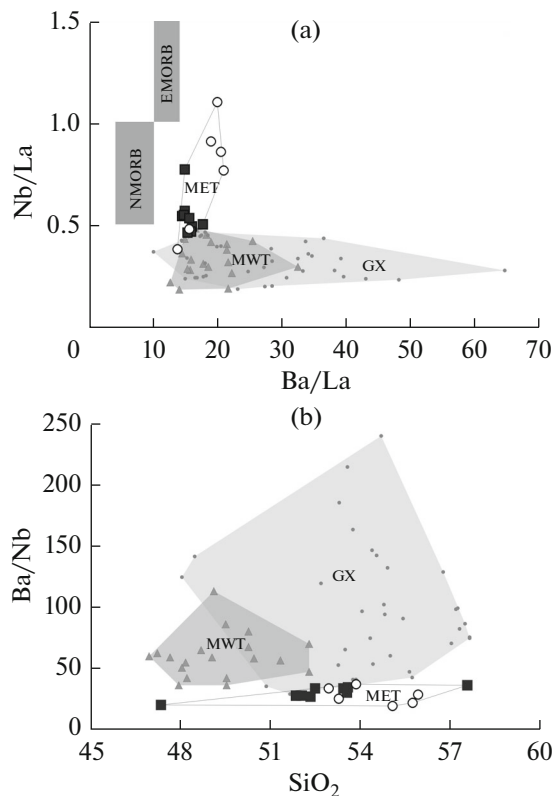


Fig. 9. The Nb/La–Ba/La (a) and Ba/Nb–SiO₂ (b) diagrams for the Early Cretaceous intermediate to basic rocks in the MWT, MET, and GX volcanic belts. For the legend, see Fig. 7. The GX compositions are after (Zhang et al., 2008b), the MWT compositions (Tugnui–Khilok and Uda sectors) are after (Yarmolyuk et al., 1998; Vorontsov and Yarmolyuk, 2007). The compositional fields for mid-ocean ridge basalts (MORB) are after (Hawkesworth et al., 1995).

the MET volcanic belt and a comparison of these with similar rocks in adjacent volcanic belts (GX on the east and the MWT on the west) suggest the following inferences:

(1) The Early Cretaceous volcanism in the Torei and Durulgui basins was fissure volcanism; faults controlled the locations and boundaries of both basins and lava sequences. Magma was mostly erupted in subaerial conditions, occasionally under water.

(2) The volcanic activity within the MET Durulgui–Torei area was long-lived, but intermittent. The Torei Lava Field was formed ~130–100 Ma ago as a result of four relatively short volcanic pulses (~130, 120, 115, and 100 Ma). Nearly the entire magma volume was erupted in the form of lava during the first two phases of the volcanism, with the subsequent subvolcanic emplacements occurring in small quantities. The volcanism in the Durulgui basin occurred generally synchronously with the TLF in the 126–94 Ma time span.

(3) The Durulgui–Torei volcanic rocks show moderate alkalinity and contain higher amounts of K₂O,

classifying them as rocks of the high potassium calc-alkaline (partly shoshonite) series. In addition, they contain high concentrations of P₂O₅ and TiO₂. The petrochemical evolutionary series of the rocks in that area is short and includes initial trachybasalts (in lower amounts), subsequent basaltic trachyandesites (dominant), and terminal trachyandesites (rare). Their origination was due to crystallization differentiation in primary basaltic magmas stored in intermediate melt reservoirs.

(4) The rocks of the area are the closest to the average OIB composition according to the concentrations of trace elements and also show an enrichment in large-ion lithophiles (Ba and K) and REEs. At the same time, the earlier lavas of the Torei Field are depleted in heavy REEs, as well as in Nb and Ta.

(5) Considered in relation to the concentration of Sr and Nd isotopes, the Durulgui–Torei rocks are moderately enriched in radiogenic strontium ($10 < \epsilon_{Sr}(t) < 21$) and slightly depleted in radiogenic neodymium ($-1 < \epsilon_{Nd}(t) < 1.5$). These distinctive features of the MET Durulgui–Torei volcanic rocks provide evidence in favor of the hypothesis that their parent magmas might come from a mantle source whose characteristics were close to the EM II. This inference is consistent with the concept of an EM II mantle that was widely abundant in Central Asia during Late Mesozoic time (Yarmolyuk et al., 1998; Yarmolyuk and Kovalenko, 2003).

ACKNOWLEDGMENTS

This work was supported by the Russian Government for the Laboratory rare-metal magmatism of IGEM RAS and the Russian Foundation for Basic Research, project no. 17-05-00167.

REFERENCES

- Afonin, V.P., Gunicheva, T.N., and Piskunova, L.F., *Rentgeno-fluorescentnyi analiz* (X-Ray Fluorescence Analysis), Novosibirsk: Nauka, 1984.
- Chernyshev, I.V., Bakharev, A.G., Bortnikov, N.S., et al., The geochronology of igneous rocks in the Nezhdanskoe Au deposit area, Yakutia, Russia: U–Pb, Rb–Sr, and Sm–Nd isotope data, *Geol. Rudn. Mestor.*, 2012, vol. 54, no. 6, pp. 487–512.
- Egorova, E., Basaltic andesites in the Torei and Borzinskoe lakes, eastern Transbaikalia, *Izv. VGGRO*, 1932, vol. 51, no. 83, pp. 1259–1268.
- Frikh-Khar, D.I. and Luchitskaya, A.I., *Pozdnemezozoiskie vulkanity i svyazannye s nimi gipabissal'nye intruzivny Mongolii* (The Late Mesozoic Volcanic Rocks and Related Hypabyssal Intrusions of Mongolia), Moscow: Nauka, 1978.
- Geologicheskoe stroenie Chitinskoi oblasti* (A Geological Map of Chita Region), An Explanatory Note to the geological map, scale 1 : 500000, Chita, 1997.

- Geologicheskaya karta Priamur'ya i sopredel'nykh territorii masshtaba 1 : 2500000* (A Geological Map of the Amur R. Area and Adjacent Territories at a Scale of 1 : 2500000), Krasnyi, L.I. and Pen Yunbiao, Editors-in-Chief, St. Petersburg, Blagoveshchensk, Harbin, 1998. *Ob'yasnitel'naya zapiska k karte* (Explanatory Note to the Map), Krasnyi, L.I., et al., Eds., 1999.
- Geologicheskaya karta Chitinskoi oblasti* (A Geological Map of Chita Region), Scale 1 : 500000, Rutshtein, I.G., Ed., Chita: PGO Chitageologiya, 1989.
- Gordienko, I.V., Klimuk, V.S., and Tsyuan Khen, The Upper Amur R. volcano-plutonic belt of East Asia, *Geol. Geofiz.*, 2000, vol. 41, no. 12, pp. 1655–1669.
- Gosudarstvennaya geologicheskaya karta Rossiiskoi Federatsii masshtaba 1 : 200000* (A Geological Map of the Russian Federation, Scale 1 : 200000), 2nd edition, Field M-50-XIV, St. Petersburg: VSEGEI, 2010.
- Hawkesworth, Ch., Turner, S., Gallagher, K., et al., Calc-alkaline magmatism, lithospheric thinning and extension in the Basin and Range, *J. of Geophysical Research*, 1995, vol. 100, pp. 10 271–10 286.
- Kelemen, P.B., Hanghøj, K., and Greene, A.R., One view of the geochemistry of subduction-related magmatic arcs, with an emphasis on primitive andesite and lower crust, in *Treatise on Geochemistry*, vol. 3, *The Crust*, Amsterdam: Elsevier, 2003, pp. 593–659.
- Klassifikatsiya magmaticheskikh (izverzhennykh) porod i slovar' terminov* (A Classification of Magmatic (Igneous) Rocks and a Glossary of Terms) Moscow: Nedra, 1997.
- Le Bas, M.J., Le Maitre, R.W., Streckeisen, A., and Zanettin, B., A chemical classification of volcanic rocks based on the total alkali-silica diagram, *J. of Petrology*, 1986, vol. 27, no. 3, pp. 745–750.
- Ogg, J.G., Ogg, G., and Gradstein, F.M., *The Concise Geologic Time Scale*, Cambridge: Cambridge University Press, 2012.
- Peccerillo, A. and Taylor, S.R., Geochemistry of Eocene calc-alkaline volcanic rocks from the Kastamonu area, Northern Turkey, *Contributions to Mineralogy and Petrology*, 1976, vol. 58, pp. 63–81.
- Petrograficheskii kodeks Rossii. Magmaticheskie, metamorficheskie, metasomaticheskie, impaktnye obrazovaniya* (Petrographic Code of Russia. Magmatic, Metamorphic, Metasomatic, and Impact Formations), 3rd Ed., rev. and suppl., St. Petersburg: VSEGEI, 2009.
- Steiger, R.H. and Jager, E., Subcommittee on geochronology: convention on the use of decay constants in geo- and cosmo-chronology, *Earth and Planet. Sci. Lett.*, 1977, vol. 36, pp. 359–362.
- Stupak, F.M., A first finding of hyaloclastites among the Late Mesozoic rocks of southern Transbaikalia, *Dokl. Akad. Nauk*, 1999, vol. 369, no. 1, pp. 92–94.
- Stupak, F.M., Core lavas—A new variety of subaqueous volcanogenic rocks, in *Petrografiya na rubezhe XXI veka (itogi i perspektivy)* (Petrography at the Turning of the 20th Century: A Summary of Results and Prospects), Syktyvkar: Geoprint, 2000, pp. 196–198.
- Stupak, F.M., The paleovolcanology of the Transbaikalian Mesozoic, in *Geologiya, Geokhimiya i Geofizika na Rubezhe XX–XXI vekov* (Geology, Geochemistry, and Geophysics at the Boundary between the 20th and 21st Centuries), Irkutsk, 2002, pp. 128–129.
- Stupak, F.M., *The hyaloclastites of the southeastern Transbaikalia*, *Zapiski Zabaikal'skogo otdeleniya Russkogo Geograficheskogo Obshchestva*, issue 131, Chita: ZO RGO, 2012, pp. 118–130.
- Vorontsov, A.A., Yarmolyuk, V.V., Ivanov, V.G., and Niki-forov, A.V., The Late Mesozoic magmatism in the Dzhida sector of the West Transbaikalia rift region: Phases of formation, associations, sources, *Petrologiya*, 2002, vol. 10, no. 5, pp. 510–531.
- Vorontsov, A.A. and Yarmolyuk, V.V., The evolution of volcanism in the Tugnui–Khilok sector of the Western Transbaikalia Rift Area in the Late Mesozoic and Cenozoic, *J. Volcanol. Seismol.*, vol. 1, no. 4, pp. 213–236.
- Vulkano-plutonicheskie assotsiatsii Tsentral'noi Mongolii* (The Volcano-Plutonic Associations of Central Mongolia) Moscow: Nauka, 1991, pp. 166–224.
- Xu, W.-L., Pei, F.-P., Wang, F., et al., Spatial–temporal relationships of Mesozoic volcanic rocks in NE China: Constraints on tectonic overprinting and transformations between multiple tectonic regimes, *J. of Asian Earth Sciences*, 2013, vol. 74, pp. 167–193.
- Yarmolyuk, V.V., Ivanov, V.G., and Kovalenko, V.I., The sources of intraplate magmatism in western Transbaikalia during Late Mesozoic to Cenozoic time: Geochemical and isotope evidence, *Petrologiya*, 1998, vol. 6, no. 2, pp. 115–139.
- Yarmolyuk, V.V. and Kovalenko, V.I., Deep geodynamics, mantle plumes and their role in the generation of the Central Asian fold belt, *Petrologiya*, 2003, vol. 11, no. 6, pp. 556–586.
- Zhang, J.-H., Gao, Sh., Ge, W.-Ch., et al., Geochronology of the Mesozoic volcanic rocks in the Great Xing'an Range, northeastern China: Implications for subduction-induced delamination, *Chemical Geology*, 2010, vol. 276, pp. 144–165.
- Zhang, J.-H., Ge, W.-Ch., Wu, F.-Yu., et al., Large-scale Early Cretaceous volcanic events in the northern Great Xing'an Range, Northeastern China, *Lithos*, 2008a, vol. 102, pp. 138–157.
- Zhang, L.-Ch., Zhou, X.-H., Ying, J.-F., et al., Geochemistry and Sr–Nd–Pb–Hf isotopes of Early Cretaceous basalts from the Great Xinggan Range, NE China: Implications for their origin and mantle source characteristics, *Chemical Geology*, 2008b, vol. 256, pp. 12–23.
- Zindler, A. and Hart, S., Chemical geodynamics, *Annual Review of Earth and Planet. Sci.*, 1986, vol. 14, pp. 493–571.

Translated by A. Petrosyan